# Analytical and Numerical Study of Pre-Stress Effect in Piezoelectric Sandwich Type Ultrasonic Transducer

**Hamidreza Nadri[1], Mahdi Shaban[2,] *, Abbas Pak[3]**
Department of Mechanical Engineering,
University of Bu-Ali Sina, Iran
E-mail: h.nadri66@gmail.com, m.shaban@basu.ac.ir, a.pak@basu.ac.ir
*Corresponding author

**Received: 20 July 2020, Revised: 1 September 2020, Accepted: 2 September 2020**

**Abstract:** In this paper, the effect of pre-stress condition on the resonance frequency of the transducer is studied by using numerical and analytical methods. To compare the obtained results, two sandwich-type transducers with nominal frequency of 25 kHz and 30 kHz are considered. Experimental determination of pre-stress value in transducer is described and measured. Then resonance frequency of transducers in the presence of pre-stress is determined by impedance analyser. Numerical analysis is conducted by modelling three-dimensional transducer in details at ABAQUS software. The resonance frequency is determined with and without pre-stress. The FE results show that by applying pre-stress on the transducers, the resonance frequency of transducers decreased. Furthermore, the FE results are very close to experimental results. Furthermore, a systematic analytical solution is presented based on one-dimensional wave propagation. The resultant displacement for each sub-section of the transducer is calculated and then all of them are assembled and solved by considering the continuity conditions of displacement and force components. It is found that pre-load condition that is produced by central bolt reduces resonance frequency of the transducer. The obtained analytical results provide fast and reliable model for predicting resonance frequency of transducer.

**Keywords:** Analytical Solution, Finite Element Analysis, Piezoelectric Ultrasonic Transducer, Pre-Stress

**Reference:** Hamidreza Nadri, Mahdi Shaban, and Abbas Pak, "Analytical and Numerical Study of Pre-Stress Effect in Piezoelectric Sandwich Type Ultrasonic Transducer", Int J of Advanced Design and Manufacturing Technology, Vol. 14/No. 1, 2021, pp. 73–81. DOI: 10.30495/admt.2021.1904847.1204

**Biographical notes: Hamidreza Nadri** received his MSc in Mechanical Engineering and currently is PhD student in Bu-Ali Sina University. His current research focuses on Advanced Manufacturing Processes and Precision Machining. **Mahdi Shaban** received his PhD in mechanical engineering from Tarbiat Modares University. His research interest includes advanced shell and plate theories, nano/micro mechanics and computational mechanics. **Abbas Pak** received his PhD in Manufacturing Engineering from Tarbiat Modares University. He is currently Assistant Professor at the Department of Mechanical Engineering, Bu-Ali Sina University, Hamedan, Iran. His current research interest includes Advanced Manufacturing Processes and Precision Machining.

 

## 1 INTRODUCTION

Ultrasonic transducers have found wide applications in various industries such as medical devices, ultrasonic cleaning, and ultrasonic welding [1]. These features can be combined with traditional machining methods to enhance accuracy and performance of them. For instance, ultrasonic machining is used for drilling of creating holes in hard and brittle ceramics [2]. Rotary ultrasonic machining is also a new technique for machining hard and brittle materials [3]. Ultrasonic vibration can assist rotating tools in incremental forming process to reduce forming force [4]. Ultrasonic welding is an effective method to increase welding quality for joining thin and dissimilar substances [5].

Typical ultrasonic transducers are manufactured by inserting piezoelectric rings between two parts, namely backing and facing and tightening by a central bolt. Both sides of piezoelectric rings are connected to electrodes to stimulate them [6]. By inserting piezoelectric rings between two metal alloys, the transducer can vibrate in resonant frequency. Pak [7] determined material properties of ultrasonic piezoelectric transducers by using Finite Element Method (FEM) and compared the obtained results with experimental modal tests. However, it is exhibited that applying compressive pre-stress loads affected the performance of the transducer. For instance, Arnold and Muhlen showed that the resonant frequency increases by increasing the pre-stress to 50 MPa [8]. Studies on the effect of pre-stress on the properties and quality of ultrasonic transducers have shown that the suitable pre-stress value for piezoelectrics is at about 30 MPa [8-9]. On the other hand, the existence of pre-stress between interfaces causes to make a proper contact surface that can significantly increase the performance of the transducer and is not neglectable [10].

Typically the pre-stress loads are created by a so-called central bolt located at the center of the transducer and is one of the important and essential components of transducers. The high yield stress materials provide a relatively smaller bolt diameter and, a lower Young's modulus does not provide suitable tightness. Thus it is recommended to use central bolt made from materials that have lower ratio value of yield stress to Young's modulus $\left({}^{\sigma_y}/_{E}\right)$ [11]. In some types of transducers, adhesive is used to provide better contact surface between piezoelectrics and central bolt, which affects the mechanical coupling coefficient [12].

It should be noted that using transducers that their length is greater than 1/4 wavelengths of resonance frequency, the one-dimensional analysis leads to a significant error [13]. The nature of pre-stress load ( i.e., compressive or tensile stress) affects the velocity of wave propagation in solids; strickly speaking compressive pre-stress in the solid environment increases wave velocity of material and tensile pre-stress decreases the wave velocity [14-15]. This effect can be seen as more evidently in materials with lower Poisson's ratio [16].

This paper aims to study the effect of pre-stress on the performance of the transducer. To this end, both numerical and analytical methods are used to predict the resonance frequency of transducer by considering pre-load effect. First, finite element method is implemented to determine resounance frequency of two manufactured transducers namely 25 kHz and 30 kHz. The Finite Element (FE) model of these transducers are build and then modal analysis is carried out by implementing bolt force. In the next step, analytical method is used to predict the resounance frequency. The one-dimensional analytical solution is carried out and the effect of pre-stress is considered. Then resonance frequency of them are measured experimentally by impedance analyzer. The results are compared with experimental results and then pros, and cons of each method are disccused.

## 2 FINITE ELEMENT ANALYSIS

In this section, the finite element method is used to investigate the effect of pre-stress in the capacity of transducer. In Ref. [1] and [6], the geometrical dimensions of 25 and 30 kHz transducers are presented, respectively in millimeter ("Figs. 1 and 2").

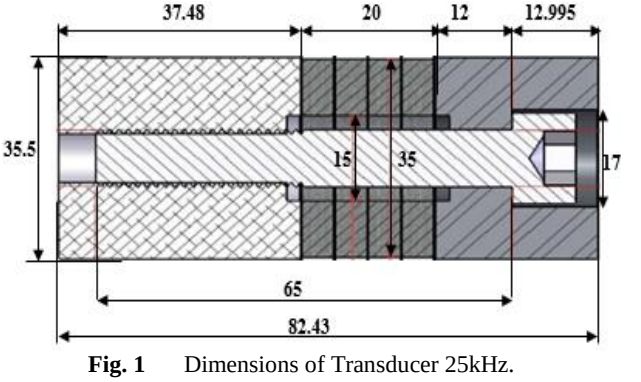


**Fig. 1** Dimensions of Transducer 25kHz.

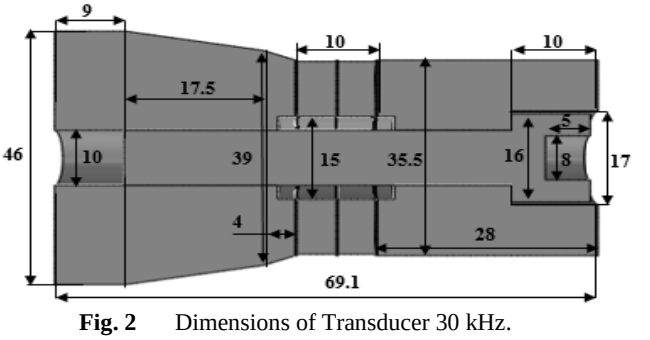


**Fig. 2** Dimensions of Transducer 30 kHz.

The corresponding material properties for each sub-sections of these two transducers are tabulated in "Table 1". The sub-sections are assembled together when applying pre-stress by a central bolt. Here the bolt load option in ABAQUS is used to consider the pre-load effect.

"Table 1" presents the mechanical properties of sub-sections used in 25 and 30 kHz transducers.

**Table 1** Material properties of sub-sections used in 25 and 30 khz transducers

| | | Material | Modulus of elasticity | Poisson ratio | Density |
|---|---|---|---|---|---|
| 25 kHz | Matching | AL 7075-T6 | 7.4426 | 0.31244 | 2823 |
| | Backing | St 304 | 20.05 | 0.2881 | 7944 |
| | Bolt (class 12.9) | St | 20.05 | 0.2881 | 7853.4 |
| | Brass Electrodes | Brass | 10.5 | 0.34 | 8484.1 |
| 30 kHz | Matching | AL 7075-T6 | 7.7 | 0.33 | 2823 |
| | Backing | St 304 | 20.7 | 0.29 | 7868 |
| | Bolt (class 12.9) | St | 20.7 | 0.29 | 7868 |
| | Brass Electrodes | Brass | 10.5 | 0.34 | 8470 |

The electro-mechanical parameters for piezoelectric rings should be considered. Piezoelectric rings of 25 kHz transducer are made from PZT-SA with ρ =7602.75 (Kg/m3). The Electrical Permeability Matrix, Piezoelectric constants and Stiffness matrix for PZT-SA by considering Y-axis as polarization axis are:

$$\left[\varepsilon_r^s\right]=\begin{bmatrix}874 & 0 & 0\\ 0 & 718 & 0\\ 0 & 0 & 874\end{bmatrix},\ [d]=\begin{bmatrix}0 & -131 & 0\\ 0 & 286 & 0\\ 0 & -131 & 0\\ 387 & 0 & 0\\ 0 & 0 & 387\\ 0 & 0 & 0\end{bmatrix}\times 10^{-12}\ m/V,$$

$$\left[S^E\right]^{-1}=\begin{bmatrix}14.8 & 8.34 & 8.28 & 0 & 0 & 0\\ 8.34 & 13.02 & 8.34 & 0 & 0 & 0\\ 8.28 & 8.34 & 14.8 & 0 & 0 & 0\\ 0 & 0 & 0 & 2.98 & 0 & 0\\ 0 & 0 & 0 & 0 & 2.98 & 0\\ 0 & 0 & 0 & 0 & 0 & 3.25\end{bmatrix}\times 10^{10}\ N/m^2$$

Furthermore, the piezoelectric pre-stress value is 27.5 MPa. Piezoelectric rings of 30 kHz transducer are made from PZT-4 with ρ=7612 (Kg/m$^3$). The Electrical Permeability Matrix, Piezoelectric constants and Stiffness matrix for PZT-4 by considering y-axis as polarization axis are:

$$\left[\varepsilon_r^s\right]=\begin{bmatrix}900 & 0 & 0\\ 0 & 600 & 0\\ 0 & 0 & 900\end{bmatrix},\ [d]=\begin{bmatrix}0 & -5.4 & 0\\ 0 & 15.8 & 0\\ 0 & -5.4 & 0\\ 12.3 & 0 & 0\\ 0 & 0 & 12.3\\ 0 & 0 & 0\end{bmatrix}\times 10^{-12}\ m/V,$$

$$\left[S^E\right]^{-1}=\begin{bmatrix}14.9 & 8.11 & 8.11 & 0 & 0 & 0\\ 8.11 & 13.2 & 8.34 & 0 & 0 & 0\\ 8.11 & 8.11 & 14.9 & 0 & 0 & 0\\ 0 & 0 & 0 & 3.13 & 0 & 0\\ 0 & 0 & 0 & 0 & 3.13 & 0\\ 0 & 0 & 0 & 0 & 0 & 3.4\end{bmatrix}\times 10^{10}\ N/m^2$$

When the central bolt fastens all parts of the transducer, compression stress is produced in sub-section parts. On the contrary, the bolt is subjected to tension stress. Two-step analysis is applied: in the first step, the bolt load is statically applied, so pre-stress is produced in the transducer. In the second step, the modal analysis is implemented to a pre-loaded transducer. It is noteworthy that the potential difference of the piezoelectric ring should be set to zero in the first step to prevent piezoelectricity that is produced due to bolt load. Here, the transducer is modeled completely in a three-dimensional space, because bolt load can be applied only

into the surface so other simplified one or two-dimensional models cannot be used. The C3D20RE element type is used for piezoelectric sections that are cubic three-dimensional element that has 20 nodes and includes electrical properties. For other sub-sections, C3D20R is used. Mesh sensitivity analysis was carried out to ensure that the results were not dependent on to the size of mesh and size of the mesh is set to 1 mm.

Figures 3 and 4 show the displacement and stress distribution of 25 kHz and 30 kHz transducers, respectively. As shown in "Figs. 3(a) and 4(a)", the location of the stationary node of vibration is in the piezoelectric section. This point has minimum displacement and is approximately at half of the transducer where there is no variation by applying pre-stress. Furthermore, the maximum displacement is in the head of matching part as anticipated. From "Figs. 3(b) and 4(b)" one can find that the central bolt is in tension while other parts are in compression. It should be noted that the stress distribution of the FE model is in accordance with Charles Mischke criterion with a 45 degree of the pattern, as shown in these figures.

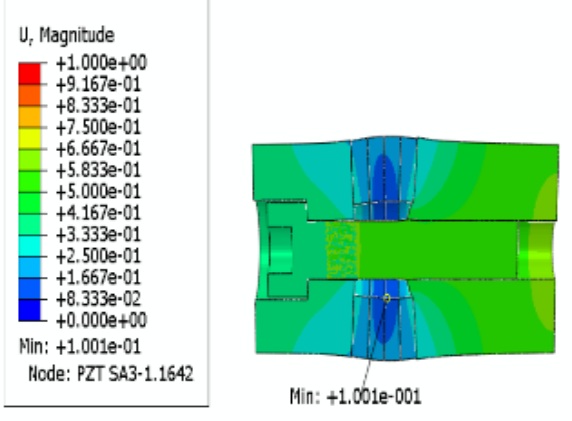


**(a)**

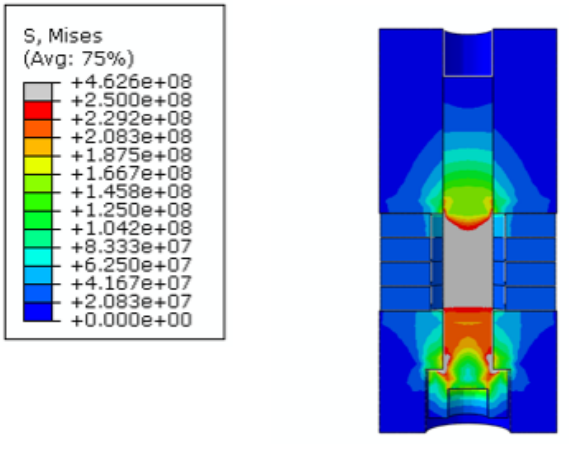


**(b)**

**Fig. 3** Stress & Displacement contour in 25 kHz transducer.

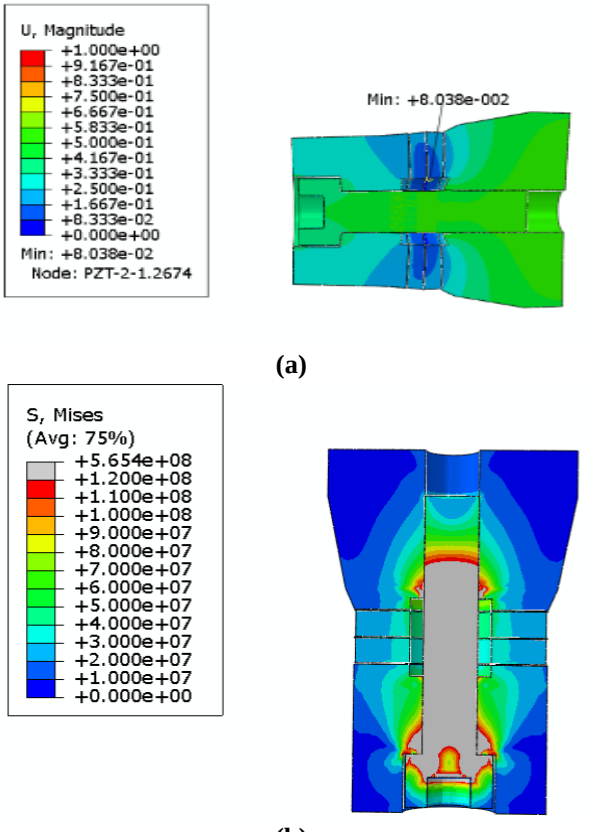


**(a)**

**(b)**

**Fig. 4** Stress & Displacement contour in 30 kHz transducer.

## 3 ANALYTICAL SOLUTION OF ULTRASONIC TRANSDUCER BY CONSIDERING PRE-STRESS EFFECT

In this section, the analytical solution of the ultrasonic transducer is studied by considering the effect of bolt pre-stress. According to material and geometric variation, the transducer is divided into several parts. The global coordinate axis, *x*, is introduced along the transducer axis, where its origin is situated on the left side of the transducer. Thus, for each part of the transducer, the one-dimensional wave propagation equation along the longitudinal axis, *x*, is as follow:

$$\frac{\partial^2 U}{\partial x^2}+\frac{1}{A}\frac{dA}{dx}\frac{\partial U}{\partial x}=\frac{1}{C_0{}^2}\frac{\partial^2 U}{\partial t^2} \quad (1)$$

Where, $U(x,t)$ is the displacement component along the $x$. $C_0$ is the phase velocity of the propagating wave ($C_0=\sqrt{\frac{E}{\rho}}$).

In this study, the Frequency Response Function (FRF) is applied to determine the resonance frequency of the transducer due to its complexity. By considering an exciting harmonic force as $f(t) = f_0 e^{i\omega t}$, and by virtue of the variable separation technique for axial displacement, $u(x.t) = u(x)f(t)$ the general solution can be obtained as:

$$u(x) = c\sin(\beta x) + c'\cos(\beta x) \tag{2}$$

Where, $\beta = \frac{\omega}{c_0}$, and ω is angular excitation frequency. It should be noted that in "Eq. (2)", the local coordinate system is adopted for subdivided parts of the transducer.

### 3.1. Case 1: The Transducer with 25 khz

As the first case, a transducer with *25 kHz* nominal resonance frequency is considered. This transducer consists of five sub-divided parts ("Fig. 5"). These sub-divided parts are matching 1, matching 2, piezoelectric, backing1, backing 2, and bolt and denoted by $M_1$, $M_2$, $P$, $b_1$, $b_2$, $S$, respectively ("Fig. 6"). Each subdivision is an annular metallic or piezoelectric ring. The central bolt is considered as a long circular bar with concentrated end mass, $m$ as bolt head [11]. In these two figures, the local coordinates are presented as $l_{M1}$, $l_{M2}$, $l_{M3}$, $l_P$, $l_{b1}$, $l_{b2}$, $l_s$, as tabulated in "Table 2". It should be noted that since the length of the matching part is greater than the length of the central bolt ($l_s$), two distinct parts are considered: $M_1$ with an annular cross-section and $M_2$ with circular solid section. Similarly, the backing part is divided into two parts $b_1$ and $b_2$ due to the existence of bolt head; thus the global coordinate of $l_{b1}$ and $l_s$ is similar.

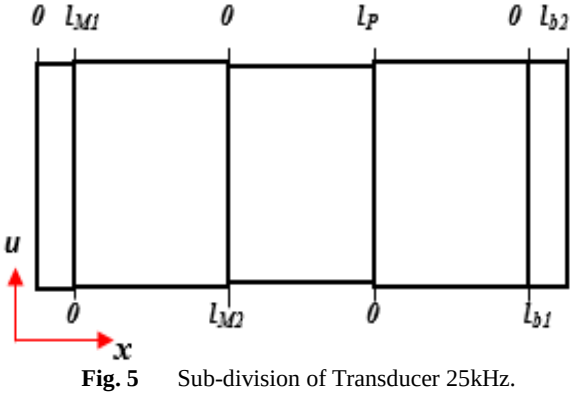


**Fig. 5** Sub-division of Transducer 25kHz.

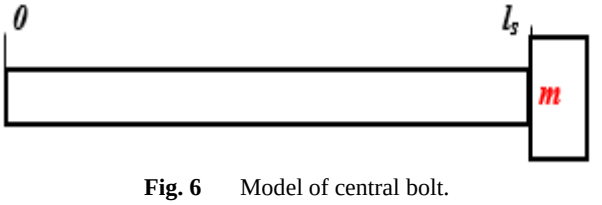


**Fig. 6** Model of central bolt.

**Table 2** local and global coordinates of 25 khz transducer (mm)

| | $M_1$ | $M_2$ | $M_3$ | p | $B_1$ | $B_2$ | S | |
|---|---|---|---|---|---|---|---|---|
| L.c | 10 | 28 | - | 20 | 12 | 13 | 60 | 25 kHz |
| G.c | 10 | 38 | - | 58 | 70 | 83 | 70 | |
| L.c | 99 | 17.5 | 44 | 10.61 | 17 | 11 | 27.62 | 30 kHz |
| G.c | 99 | 26.5 | 30.5 | 41.14 | 58.1 | 69.1 | 58.1 | |

Considering the wave propagation solution (2) in local coordinate for each sub-divided part, the following six local displacements are obtained:

$$u_{M1}(x) = c_1\sin(\beta_{M1}x) + c_2\cos(\beta_{M1}x) \tag{3}$$

$$u_{M2}(x) = c_3\sin(\beta_{M2}x) + c_4\cos(\beta_{M2}x) \tag{4}$$

$$u_s(x) = c_5\sin(\beta_s x) + c_6\cos(\beta_s x) \tag{5}$$

$$u_p(x) = c_7\sin(\beta_p x) + c_8\cos(\beta_p x) \tag{6}$$

$$u_{b1}(x) = c_9\sin(\beta_{b1}x) + c_{10}\cos(\beta_{b1}x) \tag{7}$$

$$u_{b2}(x) = c_{11}\sin(\beta_{b2}x) + c_{12}\cos(\beta_{b2}x) \tag{8}$$

Where, $c_i$, $i=1,\ldots,12$ are unknown coefficients. To determine the unknown coefficients, 12 boundary conditions is necessary. These conditions are as follow:

1- Continuity of Displacements: The following 6 boundary conditions should be satisfied at each interface to provide continuity of displacement:

$$u_{M1}(l_{M1}) = u_{M2}(0) = u_s(0) \tag{9}$$

$$u_{M2}(l_{M2}) = u_p(0) \tag{10}$$

$$u_p(l_p) = u_{b1}(0) \tag{11}$$

$$u_{b1}(l_{b1}) = u_{b2}(0) = u_s(l_s) \tag{12}$$

2- Continuity of Forces: Figure 7 presents internal forces produce in the interfaces. The forces at the junction should be balanced, thus 6 boundary conditions should be satisfied as follow:

$$f_{M1}(0)=0 \tag{13}$$

$$f_s(0)+f_{M2}(0)-f_{M1}(l_{M1})=0 \tag{14}$$

$$f_p(0)-f_{M2}(l_{M2})=0 \tag{15}$$

$$f_{b1}(0)-f_p(l_p)=-f_0 \tag{16}$$

$$f_{b2}(0)-f_s(l_s)-f_m-f_{b1}(l_{b1})=0 \tag{17}$$

$$f_{b2}(l_{b2})=0 \tag{18}$$

It is worthy to note that the inertial force of bolt head is:

$$f_m=m\frac{\partial^2 U}{\partial t^2}=-m\omega^2 u_s(l_s) \tag{19}$$

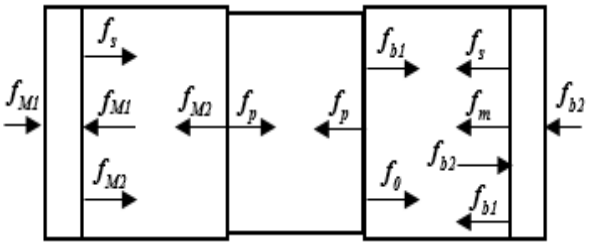


**Fig. 7** Force boundary conditions for Transducer 25 kHz.

Here, Murnaghan's theory of finite deformations is used to consider the pre-stress effect of the bolt. Based on Ref [17], the elastic Young's modulus for small strains is modified as follow:

$$E=E_0\left\{1+\frac{P}{\mu}\frac{(3\lambda+5\mu)(\lambda+2\mu)}{(3\lambda+2\mu)(\lambda+\mu)}\right\} \tag{20}$$

In the above equation, $E_0$ and $E$ are material and modified elastic modulus, respectively. $\lambda$ and $\mu$ are Lame constants. $P$ is the pressure emerged from preload bolt force. As we can conclude, the preload force changes the acoustic velocity of the body. Assembling all the above conditions, one can obtain the following system of equations:

$$C(\omega, f_0)=Q(\omega)^{-1}.B(f_0) \tag{21}$$

Where, B is force vector, $\{B\}=\{0\ \ 0\ \ 0\ \ 0\ \ 0\ \ 0\ \ 0\ \ 0\ \ 0\ \ -f_0\ \ 0\ \ 0\}^T$, C is unknown coefficients, $\{C\}=\{c_1\ \ c_2\ \ c_3\ \ c_4\ \ c_5\ \ c_6\ \ c_7\ \ c_8\ \ c_9\ \ c_{10}\ \ c_{11}\ \ c_{12}\}^T$, and $Q$ is assembled coefficient matrix. It is suitable to define transfer function, $T(\omega)$ for each part as follows:

$$T(\omega)=\frac{u(x,\omega,f_0)}{f_0} \tag{22}$$

Figure 8 plots the transfer functions of the transducer versus frequency. $T_{M1}$, $T_{M2}$, $T_p$, $T_{b1}$, $T_{b2}$ and $T_s$ are transfer functions of matching 1, matching 2, piezoelectric, backing 1, backing 2, and bolt, respectively. According to this figure, the first nominal frequency is *25.412 kHz*.

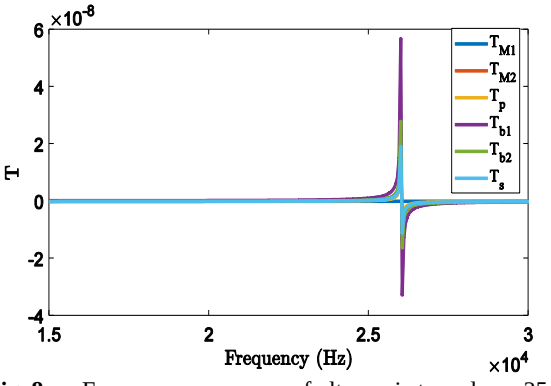


**Fig. 8** Frequency resonance of ultrasonic transducer 25 kHz with pre-stress.

### 3.2. Case 2: The Transducer with 30 khz

The 30 kHz nominal resonance frequency consists of six sub-divided parts as presented in "Fig. 9" and local and global coordinates of subdivisions are tabulated in "Table 2".

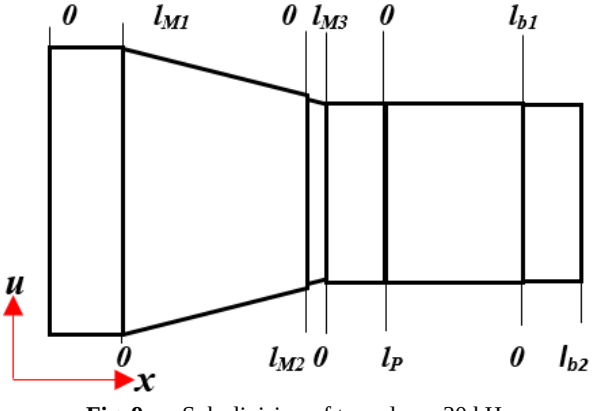


**Fig. 9** Sub-division of transducer 30 kHz.

Where, $A(x)$ is cross-section function of conic. In the mentioned transducer, the cross -section is a circle, so $A(x) = kx^2$. Considering exciting harmonic force and after some simplifications on "Eq (1)", the following wave propagation can be obtained:

$$\frac{\partial^2 u}{\partial x^2}+\frac{2}{x}\frac{\partial^2 u}{\partial x}+\beta^2 u=0 \tag{23}$$

Where, $\beta^2=\frac{\omega^2}{c_0^2}$. Equation (23) is a complex form of modified Bessel equation, and the general solution will be [18]:

$$u(x)=(\beta x)^{-1/2}\left(c_1 J_{1/2}(\beta x)+c_2 Y_{1/2}(\beta x)\right) \tag{24}$$

Where, *J* and *Y* are the first and second kinds of Bessel functions, respectively. Similar to the previous section, the following seven local displacements are obtained as follow:

$$u_{M1}(x)=c_1\sin(\beta_{M1}x)+c_2\cos(\beta_{M1}x) \tag{25}$$

$$u_{M2}(x)=x^{-1/2}\left(c_3 J_{1/2}(\beta_{M2}x)+c_4 Y_{1/2}(\beta_{M2}x)\right) \tag{26}$$

$$u_{M3}(x)=x^{-1/2}\left(c_5 J_{1/2}(\beta_{M3}x)+c_6 Y_{1/2}(\beta_{M3}x)\right) \tag{27}$$

$$u_p(x)=c_7\sin(\beta_p x)+c_8\cos(\beta_p x) \tag{28}$$

$$u_s(x)=c_9\sin(\beta_s x)+c_{10}\cos(\beta_s x) \tag{29}$$

$$u_{b1}(x)=c_{11}\sin(\beta_{b1}x)+c_{12}\cos(\beta_{b1}x) \tag{30}$$

$$u_{b2}(x)=c_{13}\sin(\beta_{b2}x)+c_{14}\cos(\beta_{b2}x) \tag{31}$$

Where, $c_i$, *i=1,…, 14* are unknown coefficients. Here 14 boundary conditions are necessary: 7 conditions for continuity of displacement and 7 conditions for force balance. Figure 10 shows the produced interface forces at the junction that should be balanced.

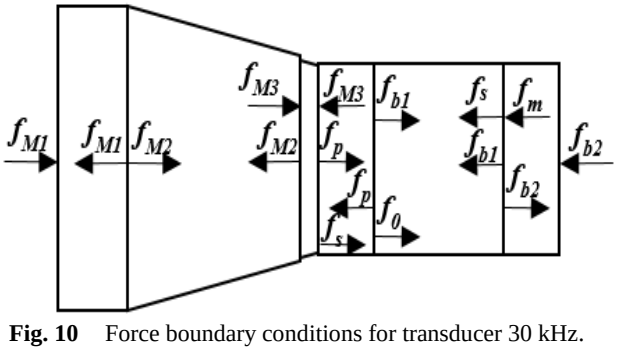


**Fig. 10** Force boundary conditions for transducer 30 kHz.

Figure 11 plots the transfer functions of the transducer versus frequency.

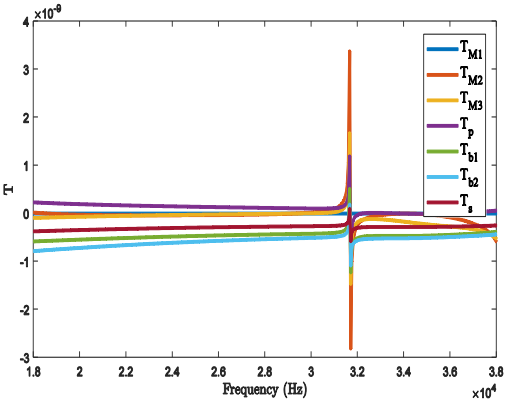


**Fig. 11** Frequency resonance of Ultrasonic Transducer 30 kHz with pre-stress.

## 4 EXPERIMENTAL RESULTS

In this section, experimental results of applying pre-stress are presented. Central bolt with the following specification is used for assembling the 25 kHz transducer: Steel Alloy M10×1.5 Class 12.9. According to Ref. [19], by considering the friction coefficient $\mu=0.15$ and pitch of *1.5 mm*, the coefficient of torsional torque $K=0.189$ for 25 kHz transducer is obtained. Thus, the tension force is obtained as:

$$F=\sigma A \tag{32}$$

The required torque applied on the bolt for fastening is:

$$T_p=K.D.F \tag{33}$$

Moreover, the obtained torque should be increased about 10 percent to compensate the looseness of the bolt after assembling.

In order to measure the actual pre-stress in central bolt experimentally, the produced charge on electrodes should be measured by volt-meter. For four piezoelectric rings made of PZT-SA, the piezoelectric and dielectric constants are $d_{33}=282\times10^{-12}\,m/V$ . $\varepsilon_{r33}^{T}=1367$. Therefore, the overall generated charge will be:

$$Q=4d_{33}\;A\;T_{OC}=24.17086\times10^{-6}C \tag{34}$$

Therefore, the overall capacitance of the transducer along with the added capacitor $C_s$ is obtained as:

$$C_{s(total)}=4C_s \tag{35}$$

And the corresponding voltage on each piezoelectric is:

$$V = \frac{Q_{total}}{C_{s(total)}} = 3250.55V \quad (36)$$

As mentioned before, applied stress is considered to be 10% higher than calculated stress; in fact, the applied stress is 30 MPa instead of 27.5 MPa. So the $Q_{total}$ is:

$$Q_{total} = 27.18 \times 10^{-6}\, C \quad (37)$$

Due to the configuration of the capacitor, the total capacitor used for Transducer 25 kHz is:

$$C_p = 45\mu F + 4C_s \quad (38)$$

Thus the measured voltage is:

$$V_0 = \frac{Q_{total}}{C_p} = 0.604V \quad (39)$$

For 30 kHz transducer with PZT-4 piezoelectric rings, the piezoelectric and dielectric constants are $d_{33} = 282 \times 10^{-12}\, m/V$ . $\varepsilon_{r33}^{T} = 1370$. Therefore, by using a capacitor with $C_p = 300\ \mu F$, the applied voltage should be $V_0 = 44.7\ mV$.

After assembling the transducer and applying pre-stress as described, the impedance analyzer is used to measure the transducer resonance frequency ("Fig. 12"). It should be noted that before measuring the resonance of transducer by Impedance Analyzer device, the piezoelectric charge must be discharged. For this purpose, two wires are connected to the negative and positive poles of the piezoelectric rings to discharged the transducer. The transducers must be tested in free (unload) conditions for more accurate results. Transducers are rested on a foam pad to decrease the environmental effects as shown in Fig. 12. According to experimental results, the measured resonance frequencies are 27.8 kHz and 23.6 kHz for 30 kHz and 25 kHz transducers, respectively.

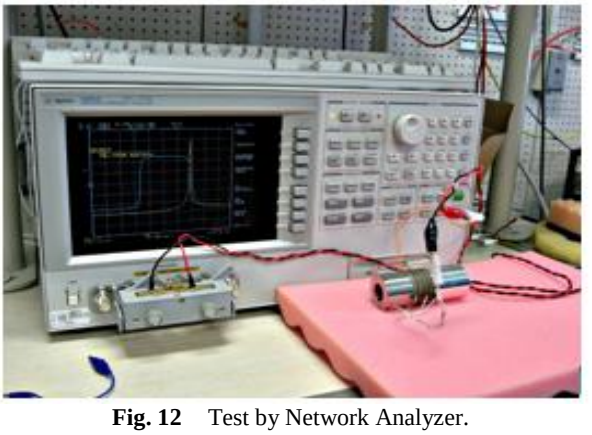

**Fig. 12** Test by Network Analyzer.

**Table 3** The results of finite element modeling, analytical solution and experimental test for transducer of 25 kHz & 30 kHz

| | 25 kHz | 30 kHz |
|---|---|---|
| (Hz) Experimental test | 23600 | 27800 |
| Analytical solution without pre-stress (Hz) | 25420 | 31675 |
| Error % Analytical solution without pre-stress | 7.71 | 13.93 |
| Analytical solution with pre-stress (Hz) | 25412 | 31671 |
| Error % Analytical solution with pre-stress | 7.67 | 13.92 |
| FEM without pre-stress (Hz) | 25204 | 30406 |
| Error % FEM without pre-stress | 6.80 | 9.37 |
| FEM with pre-stress (Hz) | 22355 | 27935 |
| Error % FEM with pre-stress | 5.27 | 0.48 |

## 5 DISCUSSION AND RESULTS

"Table 3" presents the results of finite element modeling and analytical solution for the 25 kHz and 30 kHz transducers. Also measured experimental values are presented in "Table 3". From this table one can see that by considering the pre-stress effect, the results of FE simulation are more accurate compared with experimental tests.

For a 25 kHz transducer, the error of numerical modeling without pre-stress and with pre-stress is 6.8% and 5.2%, respectively. The error value for the one-dimensional analytical solution without pre-stress and pre-stress are 7.7% and 7.6%, respectively compared with experimental test. It is seen that the error value is reduced a little by applying pre-stress in numerical modeling and the error reduction percentage is 0.1%. For 30 kHz transducer, the FE modeling error has decreased from 9.3% to 0.04% by considering pre-stress effect. It means that the predicted FE frequency becomes very accurate, and 3D modeling is very efficient.

Based on the one-dimensional analytical solution, the error has no notable change (about 1%) by considering the pre-stress effect. These results can be refined by considering lateral deformations in two or three-dimensional analysis. By extracting the stiffness matrix from FE results, it is seen that the pre-stress distribution increases and the stiffness matrix has higher values, and thus, the predicted frequency is smaller.

It is worthy to mention that applying pre-stress to transducer made a compression stress in accordance to Charles Mischke pattern, however this stress has no effect on the position of stationary point. In fact, the compression stress decreases the longitudinal displacement. The conclusions of the article are summarized as follows:

1- The pre-stress produced in assembling the transducer by central bolt reduces resonance frequency of the transducer.
2- Applying pre-stress does not change the location of the vibration stationary node of the transducer.
3- Maximum displacement occurs at the head of the matching piece when considering the pre-stress effect.
4- Applying pre-stress condition causes a decrease in displacement due to the increase of strain and stiffness of transducer.
5- The one-dimensional analysis cannot capture the pre-stress effect significantly, and the other two or three-dimensional analysis should be applied.

## REFERENCES


[1] Abdullah, A., Pak, A., Abdullah, M. M., Shahidi, A., and Malaki, M., Study of the Behavior of Ultrasonic Piezo-Ceramic Actuators by Simulations, Electronic Materials Letters, Vol. 10, No. 1, 2014, pp. 37-42. doi:10.1007/s13391-013-3098-y.

[2] Hoseini, S. M., Drilling of Engineering Ceramics Using Combination of Ultrasonic Vibrations and Diamond Slurry, Advance Design and Manufacturing Technology, Vol. 6, No. 2, 2013. http://admt.iaumajlesi.ac.ir/article_534835.html.

[3] Sadegh Amalnik, M., Expert System Approach for Optimization of Design and Manufacturing Process for Rotary Ultrasonic Machining, Advance Design and Manufacturing Technology, Vol. 11, No. 1, 2018, pp. 1-13.

[4] Amini, S., Nazari, F., Baraheni, and M., Ghasemi A. H., Investigating the Effect of Rotation Speed and Ultrasonic Vibrations in The Incremental Forming Process, Advance Design and Manufacturing Technology, Vol. 11, No. 4, 2018, pp. 91-97. http://admt.iaumajlesi.ac.ir/article_668322.html.

[5] Abdi Behnagh, R., Esmaeilzadeh, P., and Agha Mohammad Pour, M., Simulation of Ultrasonic Welding of Al-Cu Dissimilar Metals for Battery Joining, Advance Design and Manufacturing Technology, Vol 13, No. 2, 2020.

[6] Abdullah, A., Malaki, M., on The Damping of Ultrasonic Transducers' Components, Aerospace Science and Technology, Vol. 28, No. 1, 2013, pp. 31-39. doi:10.1016/j.ast.2012.10.002.

[7] Pak, A., Determination of Material Properties Components Used in Fem Modeling of Ultrasonic Piezoelectric Transducer, Advance Design and Manufacturing Technology, Vol. 12, No. 2, 2019, pp. 75-81. http://admt.iaumajlesi.ac.ir/article_668456.html.

[8] Arnold, F. J, Mühlen, S. S., Resonance Frequencies on Mechanically Pre-Stressed Ultrasonic Piezotransducers, Ultrasonics, Vol. 39, No. 1, 2001, pp. 1-5. doi:10.1016/s0041-624x(00)00047-0

[9] Arnold, F. J, Mühlen, S. S., The Influence of the Thickness of Non-Piezoelectric Pieces on Pre-Stressed Piezotransducers, Ultrasonics, Vol. 41, No. 3, 2003, pp. 191-196. doi:https://doi.org/10.1016/s0041-624x(03)00096-9.

[10] Adachi, K., Takahashi, T., and Hasegawa, H., Analysis of Screw Pitch Effects on the Performance of Bolt-Clamped Langevin-Type Transducers, the Journal of the Acoustical Society of America, Vol. 116, No. 3, 2004, pp. 1544. doi:10.1121/1.1777852.

[11] Deangelis, D. A., Schulze, G. W., and Wong, K. S., Optimizing Piezoelectric Stack Preload Bolts in Ultrasonic Transducers, Physics Procedia, Vol. 63, 2015, pp. 11-20. doi:10.1016/j.phpro.2015.03.003.

[12] Meng, X., Lin, S., Analysis of a Cascaded Piezoelectric Ultrasonic Transducer with Three Sets of Piezoelectric Ceramic Stacks, Sensors (Switzerland), Vol. 19, No. 3, 2019. doi:10.3390/s19030580

[13] Mančić, D. D., Radmanović, M. D., Design of Ultrasonic Transducers by Means of the Apparent Elasticity Method, Working and Living Environmental Protection, Vol. 2, No. 4, 2004, pp. 293-300.

[14] Tolstoy, I., On Elastic Waves in Prestressed Solids, Journal of Geophysical Research: Solid Earth, Vol. 87, No. B8, 1982, pp. 6823-6827. doi:https://doi.org/10.1029/jb087ib08p06823.

[15] Singh, I., Madan, D. K., and Gupta, M., Propagation of Elastic Waves in Prestressed Media, Journal of Applied Mathematics, 2010. doi:10.1155/2010/817680

[16] Sobieszczyk, P., Majka, M., Kuźma, D., Lim, T. C., and Zieliński, P., Effect of Longitudinal Stress on Wave Propagation in Width-Constrained Elastic Plates with Arbitrary Poisson's Ratio, Physica Status Solidi (B), Vol. 252, No. 7, 2015, pp. 1615-1619. doi:10.1002/pssb.201552256.

[17] Birch, F., The Effect of Pressure Upon the Elastic Parameters of Isotropic Solids, According to Murnaghan's Theory of Finite Strain, Journal of Applied Physics, Vol 9, No. 4, 1938, pp. 279-288. doi:10.1063/1.1710417

[18] Kreyszig, E., Advanced Engineering Mathematics, John Wiley & Sons, 2010. https://books.google.com/books?id=unn8dpxi74ec.

[19] Abdullah, A., Shahini, M., and Pak, A., An Approach to Design a High Power Piezoelectric Ultrasonic Transducer, Journal of Electroceramics, Vol. 22, No. 4, 2009, pp. 369-382. doi:10.1007/s10832-007-9408-8.